

# Spatial Cognition from Egocentric Video: Out of Sight, Not Out of Mind

Chiara Plizzari<sup>1\*</sup>, Shubham Goel<sup>2,3</sup>, Toby Perrett<sup>4</sup>, Jacob Chalk<sup>4</sup>,  
Angjoo Kanazawa<sup>3</sup>, and Dima Damen<sup>4</sup>

<sup>1</sup> Politecnico di Torino, Italy

<sup>2</sup> Avataar Inc.

<sup>3</sup> University of California, Berkeley, United States

<sup>4</sup> University of Bristol, United Kingdom

<http://dimadamen.github.io/OSNOM>

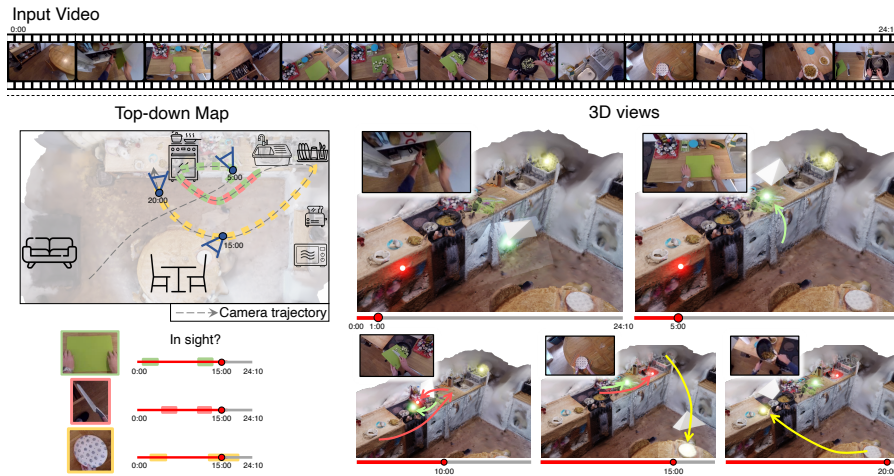


**Fig. 1: Spatial Cognition.** From an egocentric video (top), we propose the task *Out of Sight, Not Out of Mind*, where the 3D locations of all active objects are known when they are both in- and out-of-sight. We show a 24 mins video and demonstrate how solving this task enables tracking 3 active objects through the video in the world coordinate frame – from a top-view down with camera motion (left top); identifying when they are in-sight (left bottom); their trajectory from a side view at five different frames (right). Neon balls show the 3D locations of these objects over time along with the camera (white prism), corresponding frame (inset) and object location change (coloured arrow). The **chopping board** is picked from a lower cupboard (1:00) and is in-hand at 05:00. The **knife** is picked up from the drawer (after 05:00), while in use (10:00) until it is discarded in the sink (before 15:00). The **plate** travels from the drainer to the table (15:00), then back to the counter (20:00).

**Abstract.** As humans move around, performing their daily tasks, they are able to recall where they have positioned objects in their environment, even if these objects are currently out of sight. In this paper, we aim to mimic this spatial cognition ability. We thus formulate the task of *Out of Sight, Not Out of Mind* – 3D tracking active objects using

\* Work carried out during Chiara’s research visit to the University of Bristol

observations captured through an egocentric camera. We introduce Lift, Match and Keep (LMK), a method which **lifts** partial 2D observations to 3D world coordinates, **matches** them over time using visual appearance, 3D location and interactions to form object tracks, and **keeps** these object tracks even when they go out-of-view of the camera – hence keeping *in mind* what is *out of sight*. We test LMK on 100 long videos from EPIC-KITCHENS. Our results demonstrate that spatial cognition is critical for correctly locating objects over short and long time scales. E.g., for one long egocentric video, we estimate the 3D location of 50 active objects. Of these, 60% can be correctly positioned in 3D after 2 minutes of leaving the camera view.

**Keywords:** Egocentric Video · Object Tracking · 3D Understanding

## 1 Introduction

*It is lunch time and the pan is on the hob. You bend to pick the chopping board from a lower cupboard and put it on the counter. You then retrieve a knife from the cutlery drawer. You use the chopping board and knife to slide chopped food into the pan before discarding both in the sink. You then retrieve a clean plate from the drainer to serve the food. As you move around the kitchen, you are aware of where these objects are even if they are currently out of view.*

This ability to “know what is where” is an integral part of *spatial cognition*. It allows humans to build a mental map of their environment, including “memories of objects, once perceived as we moved about” [10]. Importantly, spatial cognition dictates these objects exist independently of human attention, and continue to exist in the cognitive map when the observer has left the vicinity [4, 5, 26, 52]. Spatial cognition is an innate ability, crucial to human survival, as it is how humans “acquire and use knowledge about their environment to determine where they are, how to obtain resources, and how to find their way home” [46].

In this paper, we make three prime **[C]**ontributions.

**[C1]** We introduce the task Out of Sight, Not Out of Mind (OSNOM) – maintaining the knowledge of where *all objects* are, as they are moved about and even when absent from the egocentric video stream. Egocentric views allow detailed observation of objects during interactions, e.g. the camera can look into the fridge or oven, and see exactly what was picked from the drainer in the example above. However, objects that people interact with often swiftly move out of the camera’s field of view. We focus on these challenging set of active objects that are moved by the camera wearer during the video sequence. This is distinct from the episodic memory task, e.g. [15], where the search is for one object (e.g. one’s keys), localising only when it was last seen in view. Figure 1 illustrates the OSNOM task, where the 3D location of objects and their movement is tracked throughout the video regardless of whether the objects are in view or not.

To address the OSNOM challenge, **[C2]** we propose an approach which *lifts* 2D observations to the 3D world coordinate frame – by reconstructing the scene mesh and projecting 2D detections given their depth from camera and surface

estimates. We then *match* these lifted observations using appearance and location over time to form consistent object tracks, and *keep* the knowledge of objects in mind when they are out of sight. This *lift, match and keep (LMK)* approach allows egocentric spatio-temporal understanding which humans take for granted, yet is out of reach of current methods — knowing when an object is within reach but is out-of-view, or when in-view but occluded inside a cupboard.

**[C3]** We evaluate our approach on 100 long videos from the EPIC-KITCHENS dataset [6] through past and future 3D location estimations over multiple time scales. We showcase that objects are out of view for 85% of frames on average. Using our LMK approach, we can correctly position 64% of the objects successfully after 1 minute, 48% after 5 minutes, and 37% after 10 minutes. Ablations demonstrate that maintaining 3D object locations over time is critical for correctly locating moving objects, and when they are occluded or out of view.

## 2 Related Works

**Egocentric vision** has traditionally focused on tasks within the recorded video stream, i.e. within the camera’s field of view. These include understanding actions, objects and interactions over short, and more recently longer [6, 7, 15, 42], timescales. Even when addressing future prediction (*e.g.* action anticipation [13]), memory (*e.g.* episodic memory [15]), object tracking [42], approaches scan the video stream to find when an object is in-sight. The seminal work Ego-Topo [27] builds a 2D affordance graph of the environment, relating actions to automatically discovered hotspots. The motivation to capture the relative location of an object to the camera wearer was explored in EgoEnv [28], by pre-training on 3D simulated environments. It shows that such environmentally-informed representations can improve performance on down-stream tasks such as episodic memory.

A number of tasks have been recently proposed that require 3D understanding in egocentric vision, such as jointly recognising and localising actions in a 3D map [22]. A related task to ours is Visual Query localisation in 3D (VQ3D) [15]. In VQ3D, given a query image of an object, the aim is to localise *only one* 3D position – when *the object was last seen unoccluded and in view*. Tracking is thus unnecessary (*e.g.* SOTA on VQ3D, EgoLoc [24], is based on retrieval and notes most objects are stationary). We include EgoLoc as a baseline showcasing its limitations for the OSNOM task.

**3D egocentric datasets** are now becoming available [7, 15, 16, 30, 34]. Examples include Ego4D [15], which provides 3D scans and sparse camera poses for 13% of the dataset, Ego-Exo4D [16] which captures multiple first- and third-person views, and the Aria Digital Twin [30], which contains both camera poses and object segmentation masks for its two environments. EPIC-Fields [44] provides a pipeline to extract point clouds and dense camera poses from egocentric videos, and provides camera estimates for videos from the EPIC-KITCHENS dataset [6] across 45 kitchens. We use the pipeline from EPIC-Fields [44] to localise cameras in the world coordinate frame, and VISOR masks [7] to indicate active objects.

**Object tracking through occlusion** has been investigated in 2D, where maintaining object permanence, through heuristics [17] (*e.g.* constant velocity [3]) or learning [39, 43], can help track assignment when occluded objects reappear. However, these works do not track out of the camera’s field of view, and their datasets targeting occlusion are short term, especially those with non-synthetic footage (*e.g.* TCOW [45] has a maximum video length of 464 *frames*).

**Autonomous-driving** typically maintains a map of the vehicle’s surroundings [47] and tracks nearby vehicles, even when out of sight. However, whilst they maintain locations of objects through occlusion [12, 35], tracks are deleted regularly as the vehicle only has to know about objects within its vicinity.

**Human tracking** has seen progress from 2D [1, 25, 53], to 3D [32], to 3D with motion models [14, 20, 33] which predict the location of occluded humans. Although these approaches use 3D for tracking, they usually do so in the camera coordinate frame. Some recent works have explored simultaneous reconstruction of camera motion and human pose in the 3D world coordinate frame [21, 50, 51], with [41] and [50] evaluating this concept on human tracking. [19] proposes a benchmark for tracking humans from multiple ego- and exo-centric cameras.

Our approach is related to these works for human 3D tracking. We offer the first egocentric vision work that explores tracking multiple objects in the world coordinate frame. Different from humans, objects in egocentric videos do not move by themselves, and critically move in- and out- of the camera view very frequently. We build on the human tracking approach [33], but track objects whilst taking advantage of camera localisation within the environment. Specifically, [33] tracks humans under the assumption of an external camera, thus using camera coordinates ( $x$ ,  $y$  and scale) to track humans only when they are within view. Instead, our approach is tailored for egocentric videos, with significant camera motion. As objects move out of the camera’s view frequently, tracking in 3D world coordinates maintains the notion of object permanence.

### 3 Method - Lift, Match and Keep (LMK)

Our method operates on a single untrimmed egocentric video,  $E$ , recorded in an indoor environment. We aim to keep track of all objects of interest in the 3D world coordinate frame. These 3D tracks capture where all objects are all the time, even when they are not visible in the camera frame, solving the task of Out of Sight, Not Out of Mind (OSNOM).

As many objects in the scene remain in the same position throughout the video, we focus on the challenging set of active objects that the camera wearer interacts with, typically moving these objects from one place to another, often multiple times in the video.

We take as input observations of active objects  $o_n = (f_n, m_n)$ , where  $f_n$  is a frame, and  $m_n$  is a semantic-free 2D mask in that frame given in *image coordinates*. The set of all observations, across the whole video, is  $\mathcal{O} = \{o_n : n = 1, \dots, N\}$ . We call these observations *partial*, as they do not exist for every object in every frame. The number of observations  $N$  is much larger than the number

of active objects - each object may be the subject of multiple observations.  $N$  is also independent of the number of frames  $T$ , as frames may contain zero or multiple masks.

We call our method Lift, Match and Keep (LMK). We first *lift* 2D observations of objects to 3D, *match* them over time, and *keep* objects in mind when they are out-of-sight. Section 3.1 explains how we reconstruct the global 3D representation of the static scene along with registered camera poses and monocular depth for every frame, then use this information to lift our 2D observations into the 3D world coordinate frame. Section 3.2 then takes these lifted observations and matches them in 3D across frames using distances and visual appearance similarity. Importantly for OSNOM, we maintain 3D observed positions when the objects are out of sight. Section 3.3 details how we can use knowledge from LMK to formally define object properties with respect to the camera wearer and environment. We detail LMK next.

### 3.1 Lift: Lifting 2D Observations to 3D

**3D Scene Representation.** Given a single egocentric video stream, we follow the pipeline proposed in [44] to estimate camera poses and a sparse point cloud of the static scenes. We ignore redundant frames by calculating the homography over consecutive frames, thus allowing these long videos to be processed by Structure from Motion (SfM) pipelines such as COLMAP [37]. The selected subset of video frames contains sufficient visual overlap to register all frames to the SfM point cloud and estimate a camera pose  $C_t$  for every time  $t$  in the video. Note that the intrinsic parameters of the camera are also automatically estimated by this pipeline.

This reconstruction focuses on estimating the static background of the scene. Objects in motion are deemed as outliers during matching and are accordingly ignored in the reconstructions. The pipeline produces a sparse point cloud that cannot be used for positioning objects in 3D as it is missing the notion of surfaces. We convert these point clouds to surface representations as follows.

We extract scene geometry as a 3D mesh using a classical Multi-View Stereopsis pipeline [11, 38] that runs patch matching to find dense correspondences between stereo image pairs, triangulates the correspondences to estimate depth, and fuses them together into a dense 3D point cloud with surface normals. We recover a scene mesh  $\mathcal{S}$  from the dense point cloud using Poisson surface reconstruction [18]. Examples of these meshes can be seen in Figure 1.

**Estimating 3D locations from monocular depth.** For each frame,  $f_n$ , we estimate the monocular depth estimation using [48]. The advantage of using this approach is the ability to estimate the position of both static and dynamic objects, including objects that are in-hand. However, this per-frame depth is incorrectly scaled and temporally inconsistent. We thus align it to the reconstructed 3D mesh – via a scale-shift transformation that minimises the least squares error to the mesh’s depth rendered from the estimated camera viewpoint. We refer to this as the *aligned depth map*.

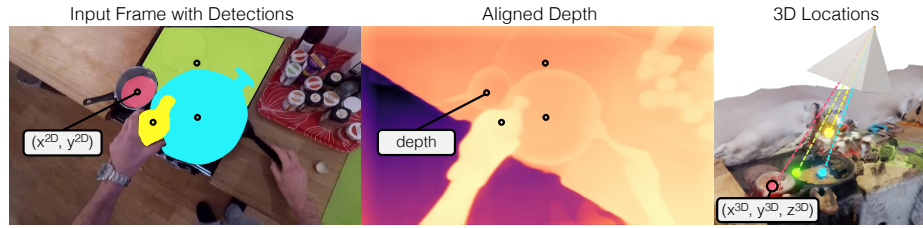


**Fig. 2: Lifting 2D observations to 3D.** We use mask centroids as 2D object locations, sample corresponding depths from the mesh-aligned monocular depth estimate. We then compute the 3D object locations in world coordinates by un-projecting the mask’s centroid from the estimated camera pose.

Given an observation  $o_n = (f_n, m_n)$ , we then assign a depth  $d_n$  to observation  $o_n$  corresponding to the centroid of the 2D mask  $m_n$  on the aligned depth map. We take the object’s 2D location in frame  $f_n$ , depth relative to the camera  $d_n$ , and camera pose  $C_{f_n}$ , and project the observation to the fixed 3D world coordinate, such that:

$$[X_n, Y_n, Z_n]^T = C_{f_n} \begin{bmatrix} d_n K^{-1} [x_n, y_n, 1]^T \\ 1 \end{bmatrix} \quad (1)$$

where  $K$  represents the camera’s intrinsic parameters. We denote this 3D location as  $l_n \in \mathbb{R}^3$ . We visualise *lifting* to 3D in Figure 2. Note that we represent each observation as a point in 3D following previous works [15, 24]. These 3D observations at this point are still partial and only on individual frames.

**Visual features.** In addition to the 3D location, we also compute visual features for each observation  $o_n$  which we need to match observations over time into 3D tracks. We denote this as  $v_n = \Psi(f_n, m_n)$ , where  $\Psi$  is a function that represents the visual feature extractor applied to the mask  $m_n$  on the frame  $f_n$ .

**Lifted Visual Observations.** We incorporate the 3D locations and visual features to give our set of partial observations  $\mathcal{W} = \{w_n : n = 1, \dots, N\}$  in the world coordinate frame, where  $w_n = (f_n, l_n, v_n)$ . We next describe how we match these observations over time to form 3D tracks.

### 3.2 Match and Keep: Matching and Keeping Lifted Observations

Given the set of lifted observations, in this section we describe how to assign observations to consistent identities (*i.e.* track objects) across time. Object permanence dictates that objects do not actually *disappear* when occluded or are out of the egocentric camera’s view – humans use spatial cognition to maintain the knowledge of where objects are.

We process the egocentric video  $E$  in an online manner. While an offline approach could also be pursued, we opt to replicate the human’s spatial cognition – *i.e.* a person only knows of an object’s location when first encountered and this is when it is kept in mind.

**Track definition.** Each track  $\mathcal{T}^j$  represents the set of observations belonging to the same object. We refer to the set of all tracks at time  $t$  as  $\mathcal{T}_t$ . A track has

one 3D location at each point in time, whether the object is in-sight or not, and we refer to the location of  $\mathcal{T}^j$  at time  $t$  by  $L(\mathcal{T}_t^j)$ .

Additionally, the track has an evolving appearance representation over time. It is calculated at time  $t$  using the visual appearance of the most recent  $\gamma$  visual features assigned to the track. Averaging visual features increases the robustness of the representation. Restricting the average to  $\gamma$  recent frames acknowledges that objects change appearance over time (*e.g.* a bowl may be full, then dirty, then clean over the course of the video). The appearance of the track at time  $t$  is denoted  $V(\mathcal{T}_t^j)$ .

**Track initialisation.** If an observation  $w_n$  represents a new, previously unseen object, i.e. is not matched to another track using the online matching described next, we initialise a new object track with this observation. We define an initialisation function  $\mathcal{I}$ , which initialises a new  $\mathcal{T}^{J+1}$ , where  $J$  tracks already exist, to the current 3D location and appearance of the observation  $w_n$ . As this is the first observation of the object, the track is projected back in time from the start of the video.  $\forall t \leq f_n$ :

$$\mathcal{I}(w_n) \rightarrow \mathcal{T}^{J+1} : L(\mathcal{T}_t^{J+1}) = l_n \text{ and } V(\mathcal{T}_t^{J+1}) = v_n \quad (2)$$

This reflects the common sense that objects do not magically appear out of thin air, so the first encounter of an object is an indication of its presence in that location earlier.

**Track update.** After a track is initialised, its visual appearance and location are updated, incorporating knowledge from new observations if they are available. We define the track update function  $\mathcal{U}$ . It takes a track, the observation which will be used to update the track, and the time, as input:

$$\mathcal{U}(\mathcal{T}^j, w_n, t) \rightarrow L(\mathcal{T}_t^j) = l_n \text{ and } V(\mathcal{T}_t^j) = \mu(v_n, \mathcal{T}^j) \quad (3)$$

where  $\mu$  calculates the mean of the past  $\gamma$  observations assigned to the track  $\mathcal{T}^j$ . If the track  $\mathcal{T}^j$  is not assigned a new observation at time  $t$  then its representation remains unchanged:  $\mathcal{U}(\mathcal{T}^j, \emptyset, t) \rightarrow \mathcal{T}_t^j = \mathcal{T}_{(t-1)}^j$ .

**Online Matching.** We describe the process of forming tracks from online observations. We find the set of new observations at each  $t$ ;  $\mathcal{W}_t = \{w_n \mid \forall n : f_n = t\}$ . Note that  $\mathcal{W}_t$  is empty if there are no observations at time  $t$ .

For the earliest frame in the video which contains at least one observation, we initialise one track for each of these  $\mathcal{T}_t = \{\mathcal{I}(w_n) \mid \forall w_n \in \mathcal{W}_t\}$ . We next iterate over every subsequent time and compare  $\mathcal{W}_t$  to the set of trajectories at time  $t - 1$ . Matching is based on a cost function using a combination of 3D distance and visual similarity. We follow [33] and model 3D similarity  $\sigma_L$  between an observation  $w_n$  and a track  $\mathcal{T}^j$  by an exponential distribution, and visual similarity  $\sigma_V$  by a Cauchy distribution:

$$\sigma_L(w_n, \mathcal{T}^j) = \frac{1}{\beta_L} \exp \left[ -D(L(\mathcal{T}_{t-1}^j), l_n) \right] \quad (4)$$

$$\sigma_V(w_n, \mathcal{T}^j) = \frac{1}{1 + \beta_V D(V(\mathcal{T}_{t-1}^j), v_n)^2} \quad (5)$$

where  $D$  is the Euclidean distance and  $\beta_L$  and  $\beta_V$  are relative weights for location and visual similarities.

We define the cost  $\Phi$  of assigning an observation with an existing track as a combination of 3D and visual distance:

$$\Phi(w_n, \mathcal{T}^j) = -\log(\sigma_L(w_n, \mathcal{T}^j)) - \log(\sigma_V(w_n, \mathcal{T}^j)) \quad (6)$$

We use the Hungarian algorithm  $\xi$ , which computes  $\Phi$  between every observation in  $\mathcal{W}_t$  and the tracks  $\mathcal{T}_{(t-1)}$ <sup>5</sup>. It returns a set of track assignments  $A_t$  for time  $t$ , where  $A_t^j = w_n$  indicates that the track  $\mathcal{T}^j$  is to be assigned the observation  $w_n \in \mathcal{W}_t$ .

$$A_t = \xi(\Phi, \mathcal{W}_t, \mathcal{T}_{t-1}) \quad (7)$$

We update the set of all tracks and initialise new tracks, such that:

$$\mathcal{T}^t \leftarrow \begin{cases} \mathcal{U}(\mathcal{T}^j, A_t^j, t) & \forall j \\ \mathcal{I}(w_n) & \forall w_n \in \mathcal{W}_t : (\nexists j : A_t^j = w_n) \end{cases} \quad (8)$$

By following the proposed online matching, we have an estimate of the 3D location for every object for which there is at least one observation.

### 3.3 LMK for object visibility and positioning

As a result of the spatial cognition enabled by the Lift-Match-and-Keep process, we are able to provide further information about the visibility of each object in relation to the camera wearer at time  $t$ . An object  $j$  can be *one* of:

- **In-sight**: if the corresponding track is assigned an observation at time  $t$ , *i.e.*  $A_t^j \neq \emptyset$
- **Occluded**: if  $L(\mathcal{T}_t^j)$  is within the field of view of the estimated camera  $C_t$ , but there is no corresponding observation ( $A_t^j = \emptyset$ ). Note that without additional knowledge we cannot distinguish between missing observations and occlusion.
- **Out-of-view**: if  $L(\mathcal{T}_t^j)$  is outside the field of view of the camera  $C_t$ .

An object may also be referred to as **Out-of-sight** if it is either out-of-view or occluded (*i.e.* in the camera’s viewing direction but cannot be detected). If an object is occluded, it is in the camera’s coverage (*i.e.* ahead of the camera wearer) but cannot be detected due to being behind or inside another object.

LMK also discloses the relative distance between the object and the camera-wearer or the static environment:

- **In-reach**: if the distance from object  $j$  to the camera’s position at time  $t$  is within the camera wearer’s near space  $\eta$ :  $D(L(\mathcal{T}_t^j), C_t) \leq \eta$
- **Out-of-reach**: as in-reach, but if  $D(L(\mathcal{T}_t^j), C_t) > \eta$ .
- **Moved**: object  $j$  has moved *relative to the environment* between times  $t_1$  and  $t_2$  if  $D(L(\mathcal{T}_{t_2}^j), L(\mathcal{T}_{t_1}^j)) \geq \epsilon$ , where  $\epsilon$  is a minimum threshold (to account for small errors in camera and object positions).
- **Stationary**: as moved, but  $< \epsilon$ .

Note that the object  $j$  at time  $t$  may be both occluded but in-reach.

<sup>5</sup> A threshold for assignment cost is set to  $\alpha$



## 4 Experiments

Section 4.1, introduces our benchmark for the OSNOM task. Section 4.2 details baseline methods. Section 4.3 contains the main results and qualitative examples. Section 4.4 ablates LMK, including its capabilities for spatial cognition.

### 4.1 Benchmarking OSNOM

**Dataset.** We evaluate on long videos from the EPIC-KITCHENS [6] dataset. This dataset offers unscripted recordings of single participants. All object motions in these videos are thus a result of the camera wearer moving objects around. We utilise the publicly available 3D point clouds and dense camera poses from EPIC-Fields [44] as well as active object masks from VISOR [7] in our method and baselines. These videos are 12 minutes long on average, containing a total of 7.9M masks, which correspond to 2939 objects. We use the object semantic label only for calculating the ground truth for evaluation.

For most of our results, we use masks provided by VISOR, which are interpolations of ground-truth masks. This allows us to assess LMK’s performance without accumulating errors from a detector. For completion, we also ablate these results with the usage of a semantic-free detector [40] in Section 4.4.

We randomly select 10 validation videos for hyperparameter tuning and 100 videos for evaluation.

**Benchmark task.** We identify a set of frames  $\mathcal{F}$  in which 3 or more objects are being interacted with. Each frame  $f \in \mathcal{F}$  includes objects that are in-sight and we wish to evaluate the methods’ ability to correctly locate the 3D locations of these same objects over frames  $f \pm \delta$ . We compare the performance of different methods as  $\delta$  increases. In total, we evaluate starting from  $\mathcal{F} = 3467$  frames, locations at 1M frames and 2171 objects, averaging 15k frames and 20 objects per video. Our benchmark will be publicly available for comparisons.

**Ground truth locations.** Note that there is no current egocentric dataset with 3D object annotations of *dynamic objects over time*. We use our 2D to 3D lifting approach presented in Section 3.1 as ground-truth locations. We assess its accuracy as follows.

We select a random set of objects and the corresponding time segments when these are in the same location throughout the environment. While we do not know the ground-truth, the error between the projections from multiple views, for the same object in the same location, is another way of assessing our 3D locations. As these are multiple instances of the same object in the same location, we can measure the mean 3D error in our 3D locations. Our analysis (details in sup-

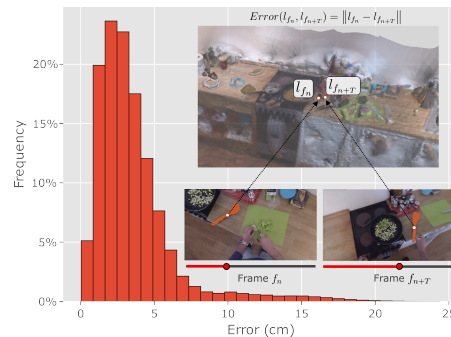


**Fig. 3: 3D Projection error.** Distribution of Euclidean distance errors for the same object, at the same location, comparing  $l_n$  to  $l_{n+T}$ .

plementary) shows that the mean 3D error is 3.5cm, with 88% of all errors smaller than 6cm and 96% of all errors smaller than 10cm (Figure 3). Given these results, we find our lifting to be sufficiently accurate to be used as ground-truth locations. This also informs our metric, where we ensure our threshold for accepting assignments is sufficiently larger than the error noted here.

**Evaluation metric.** We define a metric called Percentage of Correct Locations (PCL), drawing inspiration from the Percentage of Correct Keypoints (PCK) [49] used to evaluate pose estimation, to evaluate the spatial alignment of objects. Traditional tracking metrics do not evaluate tracks when out of sight [2, 23, 36]. PCL instead considers a predicted 3D location correct if the Euclidean distance to its ground truth 3D location is less than a threshold  $R$ .

For our main experiments, we use  $R = 30\text{cm}$ <sup>6</sup>. This reflects that a function of spatial cognition is to know the location of an object with sufficient precision in order to navigate to or obtain it [10, 46].  $R$  is visualised and ablated.

## 4.2 Experimental setup

**Baselines.** As no prior works have attempted the OSNOM task, we compare LMK against four baselines:

- **Random Matching:** each observation is randomly assigned either to an existing track or a new track, demonstrating the complexity of the data.
- **Out of Sight, Lost (OSL):** objects are forgotten when they go out-of-view, so PCL is reported as 0 and their tracks are terminated. This baseline highlights the challenge in egocentric video, where objects move very frequently out of view soon after being first observed.
- **Out of sight, out of mind (OSOM):** observations can only be assigned to tracks which are in-view. When a track goes out-of-view, PCL is reported as 0 and tracks are frozen until it is back in-view. This is an upper bound for tracking in the camera coordinate frame.
- **EgoLoc [24]:** we adapt this SOTA VQ3D approach to OSNOM, to handle multiple objects. We use the same masks, features, 3D scene and lifting for fair and direct comparison. EgoLoc’s weighted averaging over all past observations fails for OSNOM because objects change position, so instead we take the most recent match.

**Implementation details.** For appearance features  $\Psi$  we use a DINO-v2 [29] pre-trained model. We crop each mask, scale to  $224 \times 224$  and pass to the backbone. We ablate the choice of features. We set  $\alpha = 10$ ,  $\gamma = 100$ ,  $\beta_L = 13$  and  $\beta_V = 2$  (chosen on the validation set). We compute meshes in advance, which takes 5 hours on average on one 2080Ti per video. Then for online tracking, DINOv2 operates at 30 FPS and lifting-to-3D at 200FPS on one P100. LMK runs at 1000fps on a single CPU core.

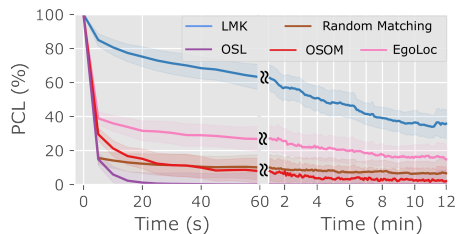


**Fig. 4: OSNOM results.** PCL of LMK compared to baselines.

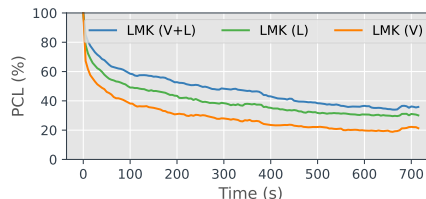


**Fig. 5: Effect of visual appearance and location.** PCL for visual features (V), location features (L), or both (V+L).

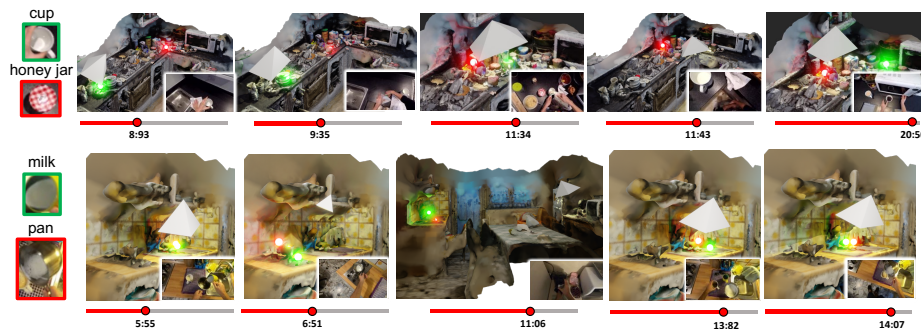


**Fig. 6: 3D location prediction.** Predicted 3D locations (Neon dots) of two objects (left) over multiple times with frame insets (right). Note how object locations are accurately kept in mind, even when the camera-wearer is far away (bottom middle).

### 4.3 Results

Results on the OSNOM task for LMK, compared to the baselines OSL, OSOM, Random Matching and EgoLoc, are shown in Figure 4. The average PCL (y-axis) over the whole dataset is reported for each 5s evaluation interval (shown on the x-axis), with standard deviation shaded. We show performance over both short (0-60 seconds) and long (1-12 minutes) timescales. Over time, the complexity of matching observations increases as more objects are being interacted with and tracked. This is reflected in performance decreasing for all methods over time.

LMK presents a significant improvement over all baselines. Compared to EgoLoc, it achieves a 39% average improvement tracking up to 1 minute, and 25% from 1 to 12 mins. This is because LMK tracks across consecutive frames, being more robust to variations in the appearance of objects due to changes in orientation or occlusion, and utilising 3D locations in the matching. The rapid drop in performance in OSOM and OSL shows the challenge of egocentric footage, where the constantly moving person causes objects to go out of view frequently. When objects are tracked until they are in-view (OSL baseline), performance goes to zero just after 20s, showing that objects are quickly lost from sight. The OSOM baseline shows that only considering objects within the camera’s field of view, without 3D world coordinates and object permanence, is insufficient for the OSNOM task (is worse than random).

<sup>6</sup> Half the standard width of a cupboard/cabinet which is 60cm/24inch

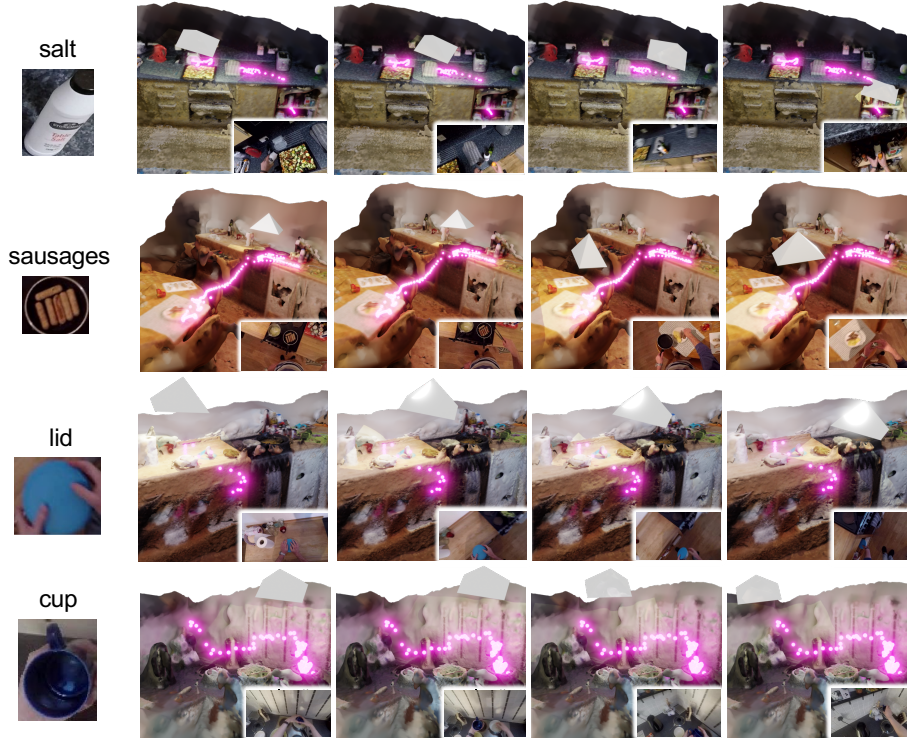


**Fig. 7: Trajectory prediction** for objects in motion. Neon dots show correctly predicted 3D positions with corresponding camera views. Objects are accurately located both when static (on surfaces) and when moving (in-hand).

**Qualitative results.** Figure 6 shows the predicted locations of a couple of objects at discrete time scales. In Figure 7, we show 3D trajectories of objects as they are moved around by the camera wearer. For example, we show the trajectory of the *salt bottle* from being in the hand (pouring salt), placed on the countertop and eventually returned to a lower cupboard, while the *cup* ends on a hanger. In all cases, LMK is capable of accurately tracking objects when when static (on surfaces) and when moving (in-hand).

#### 4.4 LMK Ablation

**Effect of visual appearance and location.** LMK assigns observations to tracks based on appearance and location similarity. Figure 5 shows the effect of only visual appearance (V) and only location (L) compared to the default of both (V+L). Their combination shows improvements (mean +19% over V, +8% over L), highlighting that appearance and location are complementary. Appearance is good for frame-to-frame assignment, and location is particularly helpful for objects in motion, occluded and for reassigning objects when they reappear.

**Accuracy at different radii.** All our experiments set the PCL threshold,  $R = 30\text{cm}$ . Figure 8 also shows results when this is increased to  $R = 60\text{cm}$

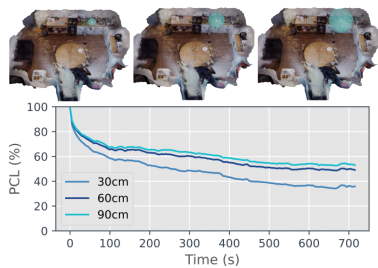


**Fig. 8: Evaluation thresholds.** LMK when increasing the PCL threshold  $R$  - the maximum distance between predicted and ground truth 3D locations considered successful. Visualisations show the regions covered by  $R = 30\text{cm}/60\text{cm}/90\text{cm}$  volumes in blue, centered on the counter.

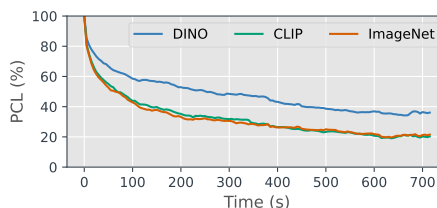


**Fig. 9: Visual feature choice** of a DINO-v2, CLIP or ImageNet (ViT).

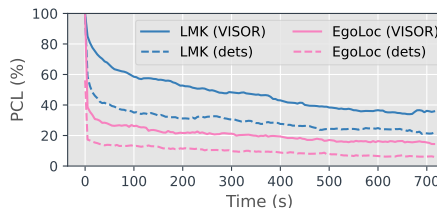


**Fig. 10: Detections.** LMK on both visual and location features when using VISOR annotations *vs* using detections from [40].

and  $R = 90\text{cm}$ , which are also visualised in 3D to show their relative difficulties. As expected, PCL increases as  $R$  increases.

**Visual features.** Our default feature extractor  $\Phi$  is a ViT [9], pre-trained under the self-supervised DINO-v2 recipe [29]. We also compare to ViTs pre-trained on CLIP [31] and ImageNet [8] in Figure 9. DINO-v2 outperforms other approaches across all timescales, likely due to the pre-training tasks of CLIP (vision and language alignment) and ImageNet (image classification) being less suited to our requirement of reliable frame-to-frame visual similarity.

**Weighting visual appearance and location.** LMK uses the hyperparameters  $\beta_V$  (Eq 4) and  $\beta_L$  (Eq 5) for relative weighting of visual and location similarities when assigning new observations to tracks. We select these based on best validation set performance averaged over timescales. Figure 11a shows validation set performance when fixing the chosen  $\beta_V = 2$  and varying  $\beta_L$ . Figure 11b fixes  $\beta_L = 13$  and varies  $\beta_V$ . Both hyperparameters are relatively stable, most likely due to the scaling by appropriate distributions (Cauchy and Exponential).

**Track visual appearance history.** Figure 11c ablates  $\gamma$  over the validation set - the number of recent features averaged for visual representation. Best results are obtained with  $\gamma = 100$ , with worse results for small / large values of  $\gamma$ , with performance relatively stable even down to only one observation.

**Detections.** We used annotations from VISOR [7] as 2D masks. This avoids compounding detector error when evaluating the error of 3D location estimation, which is our primary task. In Figure 10 we show an ablation using detections from [40]. This model provides semantic-free bounding boxes of active objects, which we use as input to LMK and the best performing baseline EgoLoc. LMK still outperforms EgoLoc by a large margin.

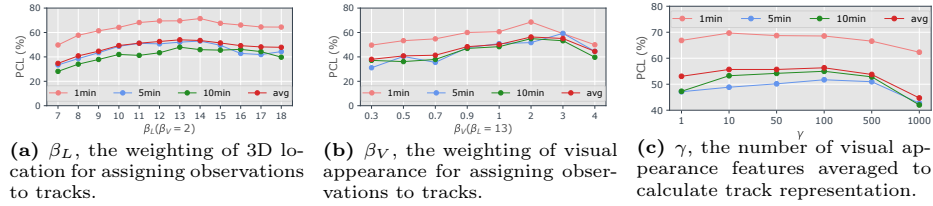


**Fig. 11: Hyperparameter ablations** for LMK on the validation set. We choose the best average over 1, 5 and 10 minute sequence lengths.

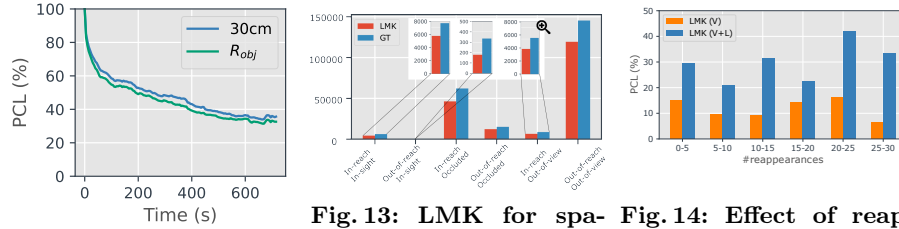


**Fig. 12: Object radius.** LMK when using approximating objects as spheres in 3D and using object radius for PCL threshold R.

**Fig. 13: LMK for spatial cognition.** Number of objects correctly located by LMK, separately by combinations of (In-reach, Out-of-reach) and (In-sight, Occluded, Out-of-view).

**Fig. 14: Effect of reappearing.** Evaluation is performed over 10 minutes, for LMK with visual appearance (V) and the combination of visual appearance and location (V+L).

**Object dimension.** In our experiments, we use a fixed  $R = 30cm$ . As objects differ in size, one might argue that matching  $R$  to the object size is more reasonable. In Figure 12 we use an adapted  $R$  that matches the object dimension per example. Results are extremely similar to the default  $R = 30cm$ .

**LMK for spatial cognition.** Figure 13 shows performance of LMK on the object states defined in Section 3.3. For each combination of (In-reach<sup>7</sup>, Out-of-reach), (In-sight, Occluded, Out-of-view), we report the total number of ground truth objects and the number LMK correctly locates over a 1 minute interval. After 1 minute of objects being interacted with, LMK is still able to determine their locations, with an average accuracy of 72%. Additionally, LMK obtains 82% on objects which are out-of-reach and out-of-view.

**Effect of objects going out-of-view.** We investigate the effect of a track going out- then back in-view (*i.e.* reappearing) within 10 minutes (Figure 14). LMK, matching using 3D locations, shows considerable performance improvement.

## 5 Conclusion

In this paper, we introduced the task of “Out of Sight, Not Out of Mind” (OS-NOM) for egocentric video with partial object observations. It evaluates 3D tracking performance of active objects when they are both in- and out-of-sight. We introduced Lift, Match and Keep (LMK), a method which *lifts* partial 2D observations in camera coordinates to 3D world coordinates, *matches* them over

<sup>7</sup> We use a reachable threshold  $\eta = 70cm$

time using visual appearance and 3D location, and *keeps* them in mind when they go out of sight. Results on long videos from EPIC-Kitchens show LMK delivers good results over both short (64% up to 1 minute) and long (37% for 1-12 minutes) timeframes, and that maintaining 3D world location is critical when objects go out-of-view. For future work, we will investigate whether LMK can help track objects that undergo state changes, and explore shared 3D object tracks between multiple ego- and exo-centric cameras.

**Acknowledgments.** Research at Bristol is supported by EPSRC Fellowship UMPIRE (EP/T004991/1) & PG Visual AI (EP/T028572/1). We particularly thank Jitendra Malik for early discussions and insights on this work. We also thank members of the BAIR community for helpful discussions. We acknowledge the use of University of Bristol’s Blue Crystal 4 (BC4) HPC facilities.

## References

1. Bergmann, P., Meinhardt, T., Leal-Taixe, L.: Tracking without bells and whistles. In: International Conference on Computer Vision (2019) [4](#)
2. Bernardin, K., Stiefelhagen, R.: Evaluating multiple object tracking performance: the clear mot metrics. EURASIP Journal on Image and Video Processing **2008**, 1–10 (2008) [10](#)
3. Breitenstein, M.D., Reichlin, F., Leibe, B., Koller-Meier, E., Van Gool, L.: Robust tracking-by-detection using a detector confidence particle filter. In: International Conference on Computer Vision (2009) [4](#)
4. Burgess, N.: Spatial memory: how egocentric and allocentric combine. Trends in cognitive sciences **10**(12), 551–557 (2006) [2](#)
5. Committeri, G., Galati, G., Paradis, A.L., Pizzamiglio, L., Berthoz, A., LeBihan, D.: Reference frames for spatial cognition: different brain areas are involved in viewer-, object-, and landmark-centered judgments about object location. Journal of cognitive neuroscience **16**(9), 1517–1535 (2004) [2](#)
6. Damen, D., Doughty, H., Farinella, G.M., Furnari, A., Ma, J., Kazakos, E., Moltisanti, D., Munro, J., Perrett, T., Price, W., Wray, M.: Rescaling egocentric vision: Collection, pipeline and challenges for epic-kitchens-100. International Journal of Computer Vision **130**, 33–55 (2022) [3](#), [9](#)
7. Darkhalil, A., Shan, D., Zhu, B., Ma, J., Kar, A., Higgins, R., Fidler, S., Fouhey, D., Damen, D.: Epic-kitchens visor benchmark: Video segmentations and object relations. In: Advances in Neural Information Processing Systems (2022) [3](#), [9](#), [13](#)
8. Deng, J., Dong, W., Socher, R., Li, L.J., Li, K., Fei-Fei, L.: Imagenet: A large-scale hierarchical image database. In: Computer Vision and Pattern Recognition (2009) [13](#)
9. Dosovitskiy, A., Beyer, L., Kolesnikov, A., Weissenborn, D., Zhai, X., Unterthiner, T., Dehghani, M., Minderer, M., Heigold, G., Gelly, S., et al.: An image is worth 16x16 words: Transformers for image recognition at scale. In: International Conference on Learning Representations (2021) [13](#)
10. Downs, R.M., Stea, D.: Image and environment: Cognitive mapping and spatial behavior. Transaction Publishers (1973) [2](#), [10](#)
11. Furukawa, Y., Ponce, J.: Accurate, dense, and robust multiview stereopsis. IEEE transactions on pattern analysis and machine intelligence **32**(8), 1362–1376 (2009) [5](#)

12. Gilroy, S., Jones, E., Glavin, M.: Overcoming occlusion in the automotive environment—a review. *IEEE Transactions on Intelligent Transportation Systems* **22**(1), 23–35 (2019) [4](#)
13. Girdhar, R., Grauman, K.: Anticipative video transformer. In: *International Conference on Computer Vision* (2021) [3](#)
14. Goel, S., Pavlakos, G., Rajasegaran, J., Kanazawa\*, A., Malik\*, J.: Humans in 4D: Reconstructing and tracking humans with transformers. In: *International Conference on Computer Vision* (2023) [4](#)
15. Grauman, K., Westbury, A., Byrne, E., Chavis, Z., Furnari, A., Girdhar, R., Hamburger, J., Jiang, H., Liu, M., Liu, X., et al.: Ego4d: Around the world in 3,000 hours of egocentric video. In: *Computer Vision and Pattern Recognition* (2022) [2](#), [3](#), [6](#)
16. Grauman, K., Westbury, A., Torresani, L., Kitani, K., Malik, J., Afouras, T., Ashutosh, K., Baiyya, V., Bansal, S., Boote, B., Byrne, E., Chavis, Z., Chen, J., Cheng, F., Chu, F.J., Crane, S., Dasgupta, A., Dong, J., Escobar, M., Forigua, C., Gebreselasie, A., Haresh, S., Huang, J., Islam, M.M., Jain, S., Khirodkar, R., Kukreja, D., Liang, K.J., Liu, J.W., Majumder, S., Mao, Y., Martin, M., Mavroudi, E., Nagarajan, T., Ragusa, F., Ramakrishnan, S.K., Seminara, L., Somayazulu, A., Song, Y., Su, S., Xue, Z., Zhang, E., Zhang, J., Castillo, A., Chen, C., Fu, X., Furuta, R., Gonzalez, C., Gupta, P., Hu, J., Huang, Y., Huang, Y., Khoo, W., Kumar, A., Kuo, R., Lakhavani, S., Liu, M., Luo, M., Luo, Z., Meredith, B., Miller, A., Oguntola, O., Pan, X., Peng, P., Pramanick, S., Ramazanov, M., Ryan, F., Shan, W., Somasundaram, K., Song, C., Southerland, A., Tateno, M., Wang, H., Wang, Y., Yagi, T., Yan, M., Yang, X., Yu, Z., Zha, S.C., Zhao, C., Zhao, Z., Zhu, Z., Zhuo, J., Arbelaez, P., Bertasius, G., Crandall, D., Damen, D., Engel, J., Farinella, G.M., Furnari, A., Ghanem, B., Hoffman, J., Jawahar, C.V., Newcombe, R., Park, H.S., Rehg, J.M., Sato, Y., Savva, M., Shi, J., Shou, M.Z., Wray, M.: Ego-Exo4D: Understanding Skilled Human Activity from First- and Third-Person Perspectives (2023) [3](#)
17. Huang, Y., Essa, I.: Tracking multiple objects through occlusions. In: *Computer Vision and Pattern Recognition* (2005) [4](#)
18. Kazhdan, M., Bolitho, M., Hoppe, H.: Poisson surface reconstruction. In: *Eurographics Symposium on Geometry Processing* (2006) [5](#)
19. Khirodkar, R., Bansal, A., Ma, L., Newcombe, R., Vo, M., Kitani, K.: Egohumans: An egocentric 3d multi-human benchmark. *International Conference on Computer Vision* (2023) [4](#)
20. Khurana, T., Dave, A., Ramanan, D.: Detecting invisible people. In: *International Conference on Computer Vision* (2021) [4](#)
21. Kocabas, M., Yuan, Y., Molchanov, P., Guo, Y., Black, M.J., Hilliges, O., Kautz, J., Iqbal, U.: Pace: Human and camera motion estimation from in-the-wild videos. *International Conference on 3D Vision* (2023) [4](#)
22. Liu, M., Ma, L., Somasundaram, K., Li, Y., Grauman, K., Rehg, J.M., Li, C.: Ego-centric activity recognition and localization on a 3d map. In: *European Conference on Computer Vision*. Springer (2022) [3](#)
23. Luiten, J., Osep, A., Dendorfer, P., Torr, P., Geiger, A., Leal-Taixé, L., Leibe, B.: Hota: A higher order metric for evaluating multi-object tracking. *International Journal of Computer Vision* **129**, 548–578 (2021) [10](#)
24. Mai, J., Hamdi, A., Giancola, S., Zhao, C., Ghanem, B.: Localizing objects in 3d from egocentric videos with visual queries. *International Conference on Computer Vision* (2023) [3](#), [6](#), [10](#)



25. Meinhardt, T., Kirillov, A., Leal-Taixe, L., Feichtenhofer, C.: Trackformer: Multi-object tracking with transformers. In: *Computer Vision and Pattern Recognition (2022)* 4
26. Moore, M.K., Meltzoff, A.N.: Object permanence after a 24-hr delay and leaving the locale of disappearance: the role of memory, space, and identity. *Developmental Psychology* 40(4), 606 (2004) 2
27. Nagarajan, T., Li, Y., Feichtenhofer, C., Grauman, K.: Ego-topo: Environment affordances from egocentric video. In: *Computer Vision and Pattern Recognition (2020)* 3
28. Nagarajan, T., Ramakrishnan, S.K., Desai, R., Hillis, J., Grauman, K.: Egocentric scene context for human-centric environment understanding from video. *Advances in Neural Information Processing Systems (2023)* 3
29. Oquab, M., Darcet, T., Moutakanni, T., Vo, H., Szafraniec, M., Khalidov, V., Fernandez, P., Haziza, D., Massa, F., El-Nouby, A., et al.: Dinov2: Learning robust visual features without supervision. *Transactions on Machine Learning Research (2024)* 10, 13
30. Pan, X., Charron, N., Yang, Y., Peters, S., Whelan, T., Kong, C., Parkhi, O., Newcombe, R., Ren, Y.C.: Aria digital twin: A new benchmark dataset for egocentric 3d machine perception. In: *International Conference on Computer Vision (2023)* 3
31. Radford, A., Kim, J.W., Hallacy, C., Ramesh, A., Goh, G., Agarwal, S., Sastry, G., Askell, A., Mishkin, P., Clark, J., et al.: Learning transferable visual models from natural language supervision. In: *International conference on machine learning (2021)* 13
32. Rajasegaran, J., Pavlakos, G., Kanazawa, A., Malik, J.: Tracking people with 3d representations. In: *Advances in Neural Information Processing Systems (2021)* 4
33. Rajasegaran, J., Pavlakos, G., Kanazawa, A., Malik, J.: Tracking people by predicting 3d appearance, location and pose. In: *Computer Vision and Pattern Recognition (2022)* 4, 7
34. Ravi, S., Climent-Perez, P., Morales, T., Huesca-Spaurani, C., Hashemifard, K., Flórez-Revuelta, F.: Odin: An omnidirectional indoor dataset capturing activities of daily living from multiple synchronized modalities. In: *Computer Vision and Pattern Recognition (2023)* 3
35. Ren, X., Yang, T., Li, L.E., Alahi, A., Chen, Q.: Safety-aware motion prediction with unseen vehicles for autonomous driving. In: *International Conference on Computer Vision (2021)* 4
36. Ristani, E., Solera, F., Zou, R., Cucchiara, R., Tomasi, C.: Performance measures and a data set for multi-target, multi-camera tracking. In: *European conference on computer vision*. Springer (2016) 10
37. Schönberger, J.L., Frahm, J.M.: Structure-from-motion revisited. In: *Conference on Computer Vision and Pattern Recognition (2016)* 5
38. Schönberger, J.L., Zheng, E., Pollefeys, M., Frahm, J.M.: Pixelwise view selection for unstructured multi-view stereo. In: *European Conference on Computer Vision (2016)* 5
39. Shamsian, A., Kleinfeld, O., Globerson, A., Chechik, G.: Learning object permanence from video. In: *European Conference on Computer Vision (2020)* 4
40. Shan, D., Geng, J., Shu, M., Fouhey, D.F.: Understanding human hands in contact at internet scale. In: *Proceedings of the IEEE/CVF conference on computer vision and pattern recognition*. pp. 9869–9878 (2020) 9, 13
41. Sun, Y., Bao, Q., Liu, W., Mei, T., Black, M.J.: Trace: 5d temporal regression of avatars with dynamic cameras in 3d environments. In: *Computer Vision and Pattern Recognition (2023)* 4

42. Tang, H., Liang, K.J., Grauman, K., Feiszli, M., Wang, W.: Egotracks: A long-term egocentric visual object tracking dataset. *Advances in Neural Information Processing Systems* **36** (2024) [3](#)
43. Tokmakov, P., Li, J., Burgard, W., Gaidon, A.: Learning to track with object permanence. In: *International Conference on Computer Vision* (2021) [4](#)
44. Tschernezki, V., Darkhalil, A., Zhu, Z., Fouhey, D., Larina, I., Larlus, D., Damen, D., Vedaldi, A.: EPIC Fields: Marrying 3D Geometry and Video Understanding. In: *Proceedings of the Neural Information Processing Systems* (2023) [3](#), [5](#), [9](#)
45. Van Hoorick, B., Tokmakov, P., Stent, S., Li, J., Vondrick, C.: Tracking through containers and occluders in the wild. In: *Computer Vision and Pattern Recognition* (2023) [4](#)
46. Waller, D.E., Nadel, L.E.: *Handbook of spatial cognition*. American Psychological Association (2013) [2](#), [10](#)
47. Wong, K., Gu, Y., Kamijo, S.: Mapping for autonomous driving: Opportunities and challenges. *IEEE Intelligent Transportation Systems Magazine* **13**(1), 91–106 (2020) [4](#)
48. Yang, L., Kang, B., Huang, Z., Xu, X., Feng, J., Zhao, H.: Depth anything: Unleashing the power of large-scale unlabeled data. *Computer Vision and Pattern Recognition* (2024) [5](#)
49. Yang, Y., Ramanan, D.: Articulated human detection with flexible mixtures of parts. *IEEE transactions on pattern analysis and machine intelligence* **35**(12), 2878–2890 (2012) [10](#)
50. Ye, V., Pavlakos, G., Malik, J., Kanazawa, A.: Decoupling human and camera motion from videos in the wild. In: *Computer Vision and Pattern Recognition* (2023) [4](#)
51. Yuan, Y., Iqbal, U., Molchanov, P., Kitani, K., Kautz, J.: Glamr: Global occlusion-aware human mesh recovery with dynamic cameras. In: *Computer Vision and Pattern Recognition* (2022) [4](#)
52. Zewald, J., Jacobs, I.: Object permanence. In: *Encyclopedia of animal cognition and behavior*, pp. 4711–4727. Springer (2022) [2](#)
53. Zhang, Y., Sun, P., Jiang, Y., Yu, D., Weng, F., Yuan, Z., Luo, P., Liu, W., Wang, X.: Bytetrack: Multi-object tracking by associating every detection box. In: *European Conference on Computer Vision*. Springer (2022) [4](#)

## Appendix

### A Estimating error in the 3D projection

In Sec 4.1, we estimate the error in 3D locations, through comparing projections of static objects from multiple viewpoint. Figure 3 in the paper presented the findings – showcasing that the mean error is 3.5cm with 96% of all errors within 10cm. We here describe the data used to report this figure.

We randomly selected 207,277 pairs of frames from our dataset, covering correspondences between 10 static objects across 5 different kitchens/environments. These were manually selected as multiple frames with masks of the same object, at distinct times, and from different viewpoints. We avoid masks that are partially occluded by another object or by the camera’s field-of-view (i.e. not fully in view) as these projections are likely to differ due to the occlusion of part of the mask. As the chosen pairs of masks showcase the same static object, their 3D locations should perfectly match. Any differences in their 3D location can be used to measure the error in the 3D projection, which we use as ground truth locations.

As the figure showcases, the error in our projections is within 10cm and well-within the threshold we use of 30cm. Recall that our threshold is chosen to reflect the cupboard width in standard kitchens. Estimating an object’s location within 30cm implies we can position the object correctly within a cupboard.

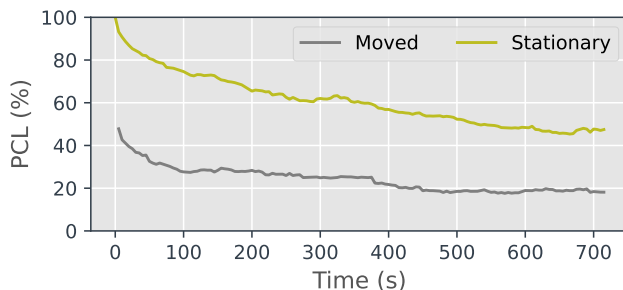


**Fig. 15:** LMK Results for **Moved vs Stationary** objects with respect to the environment.

### B Moved vs. Stationary objects

Section 3.3 also provides a definition of objects which have either moved or remained stationary with respect to the environment. Figure 15 shows PCL results using a movement threshold of  $\epsilon = 30\text{cm}$ . The performance of stationary objects is on average 35% better than that of objects which have moved. Objects are more visually different after a move (*e.g.* different orientation or lighting).

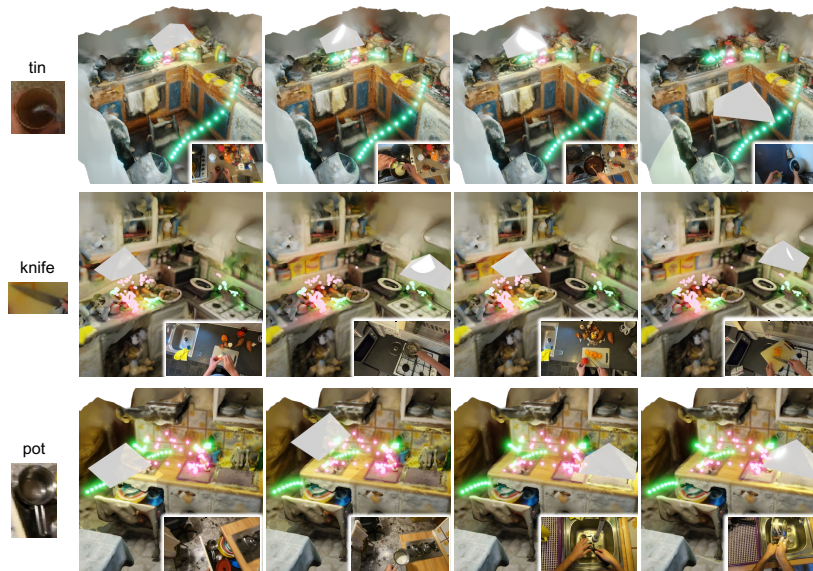


**Fig. 16: Trajectory prediction - temporarily lost but recovered track.** Predicted trajectory of three objects in motion. Green neon dots show correctly predicted 3D positions over four frames with their corresponding camera views, and red neon dots show ground-truth trajectory where the prediction fails. The tracking momentarily fails, but subsequently, the object is accurately matched to a future observation.

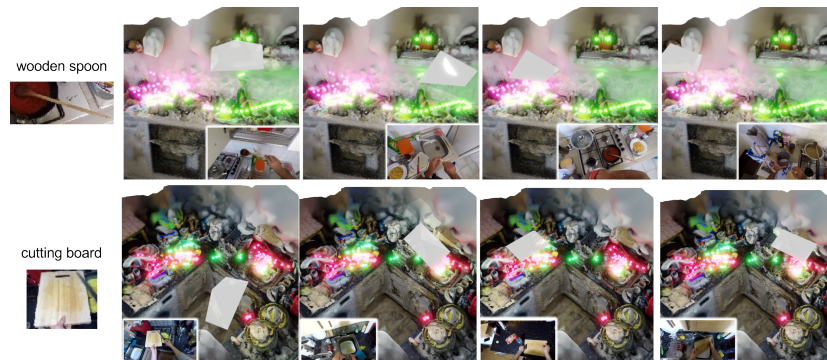


**Fig. 17: Trajectory prediction - lost track.** Predicted trajectory of two objects in motion. Green neon dots show correctly predicted 3D positions over four frames with their corresponding camera views, and red neon dots show ground-truth trajectory where the prediction fails. The tracking fails and all subsequent predictions are assigned to a new track.

## C Failure cases

We identify two key reasons for failure cases for LMK. For clarity, we showcase each case separately – in Figure 16 and Figure 17. For each figure, we focus on a single object and show its predicted trajectory in green. Failure predictions are shown in red, where we plot the correct ground truth trajectory.

In Figure 16 we show cases where the track is lost for a limited time but is then correctly recovered. In the first row, the tin is correctly tracked for most of its trajectory, including when it is discarded in the bin. However, for a short duration, the predictions are incorrect (red dots). Similarly, in the second row, the knife is incorrectly predicted while occluded by the hand or occluded in hand. The last example shows failures in predicting the correct trajectory of the pot as it is filled with milk which changes its appearance. Coincidentally, it is moved out of the field of view. The matching then fails for both the appearance and the location. As the pot is emptied, its appearance matching is recovered towards the end of the track.

In Figure 17, we show failure cases of tracking that are not recovered. In the first example, the wooden spoon is assigned a new trajectory and the tracking continues using the new identity. This is similarly the case for the cutting board when it is moved to the cluttered sink.

Failures predominantly occur in cluttered scenarios, such as when slicing peppers with a knife in Figure 16, or mixing with a spoon in Figure 17. In these situations, the locations of multiple objects overlap, making the individual object’s location less informative for matching.

## D Future Directions

We report the majority of our results using ground-truth masks out of the VISOR annotations. This allows us to evaluate the tracking from partial observations without accumulating detection errors. We find this decision to be reasonable as we focus on introducing and evaluating the task of Out of Sight, Not Out of Mind (OSNOM). In Fig 10, we ablate this by using an off-the-shelf semantic-free detector. The figure shows an expected drop in performance as noisy and incomplete detections are introduced. Improving performance using detection predictions is one of the future directions.

Another future direction is the expansion of OSNOM task to multiple videos, over time. In follow-up videos, the initial assumption of where objects are from previous sessions can be used as priors for OSNOM. Extending beyond a single video targets our ultimate goal of an assistive solution that is aware of where objects are, over hours and potentially days.